

Non-Rigid Motion Compensation for Breast CT

Mikhail Mikerov, Koen Michielsen, Nikita Moriakov, and Ioannis Sechopoulos

Abstract—The image quality in dynamic contrast-enhanced breast CT is expected to suffer from motion artifacts due to the extended acquisition time involved. We propose an iterative method for compensation of motion artifacts due to non-rigid movement of the breast. The motion vector field is approximated using b-splines on a sparse grid and its values are found by minimizing errors in the projection domain. We evaluated the method on an anthropomorphic phantom with realistic motion and visual assessment yielded a clear reduction in motion artifacts. Quantitatively, we observed an increase of the structural similarity from 0.9988 to 0.9995 and a decrease of the normalized root mean squared error from 0.1448 to 0.0932.

I. INTRODUCTION

Motion artifacts are expected to become one of the main causes of image quality degradation in dynamic contrast-enhanced (DCE) breast CT due to long acquisition times [1] needed to characterize contrast agent uptake and washout. These artifacts will not only make the analysis of images by radiologists more difficult, but will also limit the quantitative accuracy that is necessary for automatic data analysis. Hence, a motion compensation method is required to avoid these pitfalls. Earlier we demonstrated that the expected motion of the breast during DCE breast CT imaging is non-rigid and does not necessarily exhibit periodic patterns [2]. On the contrary, it is expected that the breast will undergo sudden and rather abrupt movements, making the application of motion compensation methods that assume specific motion trajectories not applicable [3].

In this work, we propose a method for non-rigid motion compensation for breast CT that does not require any prior knowledge about the motion and uses b-splines to represent the motion vector field. The b-spline parameters are updated using gradient descent by minimizing a loss function in the projection domain. We demonstrate the feasibility of our method on an anthropomorphic phantom with realistic known motion obtained from DCE-MRI sequences.

II. MATERIALS AND METHODS

A. Deformable image resampling

In this work we opted to approximate motion using cubic b-splines since they provide a good trade-off between being able to capture the motion and computational complexity. Given

This study was supported by ERC grant 864929.

All authors are with the Department of Medical Imaging, Radboudumc, Nijmegen, The Netherlands, e-mail: mikhail.mikerov@radboudumc.nl.

N. Moriakov is with the Department of Radiation Oncology, Netherlands Cancer Institute, Amsterdam, The Netherlands

I. Sechopoulos is with the Dutch Expert Center for Screening (LRCB), Nijmegen, The Netherlands and with the Technical Medicine Center, University of Twente, Enschede, The Netherlands

a motion field, we can resample the volumes in the image domain using spatial transformers – differentiable modules to apply spatial transformations when training neural networks with gradient descent introduced by Jaderberg et al. [4]. The main component of a spatial transformer is a flow-field grid of the same dimensionality as the image, which specifies the locations of pixels in the original image that need to be used to create a pixel value in the transformed image. In case of 3D volumes, one would require three 3D grids, one for deformation along each axis. Rigid transformations can be effectively represented using such grids since all voxels move in the same way. However, it is also possible to apply deformable image resampling using the same idea by populating the flow-field grid with the corresponding values.

B. Combined motion estimation and compensation

Our method is inspired by the joint motion estimation and compensation method of Sun et al. [5] with the major difference being that we resample in the image domain instead of virtually shifting the detector. The modified estimation and compensation algorithm works as follows: the b-spline coefficients B_p in the form of a three-channel 3D tensor for each projection p are initialized with zeros (i.e., no motion present), and the projection data P are reconstructed using FDK without any corrections, generating image I . For each iteration of the joint algorithm, motion is then estimated sequentially for all projections $p \in P$ so that the data can fit in GPU memory. To update the estimated motion B_p , the reconstruction is deformed using the spatial transformer introduced in the previous section with the current b-spline coefficients, and reprojected. The coefficients are then updated by gradient descent to minimize the mean squared error (MSE) in the projection. After this procedure has been performed for all projections, a new FDK reconstruction is performed using the updated motion represented in the b-spline coefficients.

C. Evaluation on an anthropomorphic phantom

We tested the performance of our method on a previously developed anthropomorphic phantom with known motion [2]. In short, real non-rigid patient motion was obtained by registering subsequent frames in a DCE-MRI sequence. Next, the motion was parameterized in time using a sigmoid function to simulate abrupt motion during a scan. In this evaluation, the motion occurred during acquisition of projections 125–175 out of 300 in one full revolution. Finally, the obtained motion vector field was applied to a digital phantom followed by forward projection of the phantom at each projection time point. The detector’s dimensions were 700x200 pixels, the reconstructed volume was 300x500x500 voxels. At each time point, the motion was represented by 17x27x27 b-spline

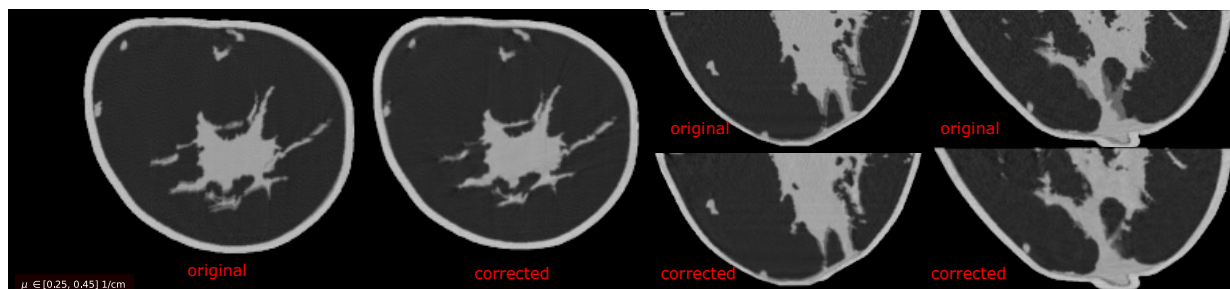


Fig. 1. Breast CT reconstruction of anthropomorphic phantom that underwent non-rigid motion during acquisition. The reconstruction with motion compensation is shown on the right for coronal plane, and on the bottom for sagittal and transverse planes.

coefficients for each direction, resulting in approximately 11 million parameters needed to be estimated. The method was stopped after three iterations.

III. RESULTS

Figure 1 shows the comparison of images reconstructed with and without our motion compensation. Noticeable changes are the removal of ghosting of fine structures and sharpening of the edges between fibro-glandular and adipose tissues. Moreover, the correct skin line profile is recovered. Using the reconstruction of the ground truth phantom without added motion as the reference image, the structural similarity index (SSIM) in the whole volume (window size $3 \times 3 \times 3$ voxels) improved from 0.9988 to 0.9995. Figure 2 shows that the SSIM increases for all slices. Likewise, the normalized root mean squared error (RMSE) compared to the reference image decreased from 0.1448 to 0.0932.

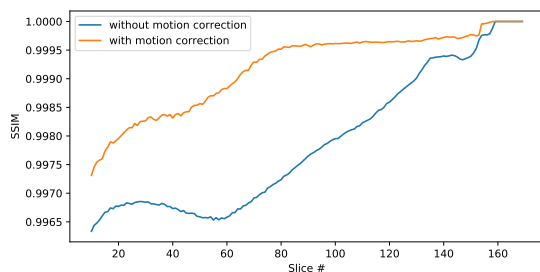


Fig. 2. SSIM as a function of slice number for reconstructed volumes with and without motion compensation compared to the ground truth phantom with no motion.

IV. DISCUSSION

Both qualitative and quantitative analysis indicate improvement of the image quality after motion compensation. This indicates that the b-spline based motion field can represent the non-rigid motion captured from patient data. Additionally, we find that the method converges quickly to the correct motion representation. It should be noted that a denser grid of b-spline coefficients will likely slow down the convergence since more parameters need to be optimized. The number of parameters used to describe the motion in the evaluation was not optimized, but based on our results it appears the selected grid was sufficiently dense.

The runtime of a single iteration of the method was found to be 0.8 s to estimate the motion for a single projection and about 4 minutes to perform motion-compensated FDK on an Nvidia A6000 GPU, for a total of approximately 24 minutes for 3 iterations. The runtime could be further improved both by moving to a more efficient implementation and by using a multiresolution approach.

A potential drawback of our method is the resolution loss due to multiple resampling in the image domain; once in the ray tracer to calculate the forward and backward projections, and once in the spatial transformation to apply the motion. Although we did not observe this effect with our phantom, it could be more obvious with real patient data, and we plan to avoid this in the future by adding the motion transformation to the ray tracer.

V. CONCLUSION

We developed a non-rigid motion compensation method for breast CT. The main advantage of our method is the ability to remove motion artifacts that originate due to fast non-rigid movement of the breast in the field of view and do not necessary exhibit certain motion patterns that can be approximated by a model.

REFERENCES

- [1] L. Brombal, L. M. Arana Peña, F. Arfelli, R. Longo, F. Brun, A. Contillo, F. Di Lillo, G. Tromba, V. Di Trapani, S. Donato, R. H. Menk, and L. Rigon, "Motion artifacts assessment and correction using optical tracking in synchrotron radiation breast ct," *Medical Physics*, vol. 48, no. 9, pp. 5343–5355, 2021. [Online]. Available: <https://aapm.onlinelibrary.wiley.com/doi/abs/10.1002/mp.15084>
- [2] M. Mikerov, K. Michielsen, N. Moriakov, and I. Sechopoulos, "Adding patient motion from DCE-MRI to anthropomorphic phantoms for dedicated breast CT," in *Medical Imaging 2022: Image Processing*, vol. 12032. SPIE, 2022, pp. 570 – 575. [Online]. Available: <https://doi.org/10.1117/12.2611487>
- [3] Q. Tang, J. Cammin, S. Srivastava, and K. Taguchi, "A fully four-dimensional, iterative motion estimation and compensation method for cardiac ct," *Medical Physics*, vol. 39, no. 7Part1, pp. 4291–4305, 2012. [Online]. Available: <https://aapm.onlinelibrary.wiley.com/doi/abs/10.1118/1.4725754>
- [4] M. Jaderberg, K. Simonyan, A. Zisserman, and k. kavukcuoglu, "Spatial transformer networks," in *Advances in Neural Information Processing Systems*, C. Cortes, N. Lawrence, D. Lee, M. Sugiyama, and R. Garnett, Eds., vol. 28. Curran Associates, Inc., 2015.
- [5] T. Sun, J.-H. Kim, R. Fulton, and J. Nuyts, "An iterative projection-based motion estimation and compensation scheme for head x-ray ct," *Medical Physics*, vol. 43, no. 10, pp. 5705–5716, 2016. [Online]. Available: <https://aapm.onlinelibrary.wiley.com/doi/abs/10.1118/1.4963218>